Chemistry & Biology
Article

Engineered Synthesis of 7-Oxo- and 15-Deoxy-15-Oxo-Amphotericins: Insights into Structure-Activity Relationships in Polyene Antibiotics

Patrick Power,[1] Terence Dunne,[1] Barry Murphy,[1,3] Laura Nic Lochlainn,[1] Dilip Rai,[1] Charles Borissow,[2] Bernard Rawlings,[2] and Patrick Caffrey[1,*]
[1]School of Biomolecular and Biomedical Science and Centre for Synthesis and Chemical Biology, University College Dublin, Belfield, Dublin 4, Ireland
[2]Department of Chemistry, University of Leicester, University Road, Leicester LE1 7RH, United Kingdom
[3]Present address: Department of Chemistry, University of Leicester, University Road, Leicester LE1 7RH, United Kingdom.
*Correspondence: patrick.caffrey@ucd.ie
DOI 10.1016/j.chembiol.2007.11.008

SUMMARY

Site-directed mutagenesis and gene replacement were used to inactivate two ketoreductase (KR) domains within the amphotericin polyketide synthase in *Streptomyces nodosus*. The KR12 domain was inactivated in the Δ*amphNM* strain, which produces 16-descarboxyl-16-methyl-amphotericins. The resulting mutant produced low levels of the expected 15-deoxy-15-oxo analogs that retained antifungal activity. These compounds can be useful for further chemical modification. Inactivation of the KR16 domain in the wild-type strain led to production of 7-oxo-amphotericin A and 7-oxo-amphotericin B in good yield. 7-oxo-amphotericin B was isolated, purified, and characterized as the *N*-acetyl methyl ester derivative. 7-oxo-amphotericin B had good antifungal activity and was less hemolytic than amphotericin B. These results indicate that modification at the C-7 position can improve the therapeutic index of amphotericin B.

INTRODUCTION

Amphotericin B is a medically important antifungal antibiotic that is produced by *Streptomyces nodosus* (Lemke et al., 2005). Like other polyene macrolides, amphotericin B acts by interacting selectively with ergosterol in fungal cells to form transmembrane channels. Amphotericin B has several other biological activities that result from interactions with sterols in other cell membranes. It is active against enveloped viruses, protozoan parasites, and pathogenic prion proteins (Lemke et al., 2005; Hartsel and Bolard, 1996). Low doses of amphotericin B reactivate the latent state of HIV in macrophages, and could deplete pools of proviruses that are insensitive to antiretroviral drugs (Jones et al., 2005). When administered as a drug, amphotericin B has serious side effects, primarily nephrotoxicity, due to its low water solubility, interactions with cholesterol in human cell membranes, and its facile oxidation to form reactive species that damage cells (Abu-Salah, 1996; Schaffer, 1984). The considerable and wide-ranging therapeutic potential of amphotericin B has not been fully exploited because of its toxicity. The adverse effects can be moderated by encapsulating the drug in liposomes or lipid complexes (Lemke et al., 2005). However, these lipid formulations have residual toxicity and their use is limited by their expense. With the rapid worldwide increase in incidence of life-threatening systemic fungal infections, there is an urgent need for a commercially viable nontoxic analog of amphotericin B that retains its antifungal activity.

Several analogs have been made by chemical modification of the natural product. These have provided the first insights into structure-activity relationships and indicate how toxicity might be reduced. The series of conjugated double bonds is essential for antibiotic activity (Cereghetti and Carreira, 2006). Suppression of charge on the exocyclic carboxyl group increases specificity for ergosterol over cholesterol (Cheron et al., 1988). Derivatization of mycosamine can improve the therapeutic index, provided that the amino group retains a positive charge (Szlinder-Richert et al., 2001; Paquet and Carreira, 2006; Ehrenfreund-Kleinman et al., 2002). Modification at the C-13 hemiketal reduces hemolytic activity with a slight decrease in antifungal activity (Taylor et al., 1992). Fluorine atoms introduced at C-14 or C-28 do not affect activity, and will be valuable in detailed studies of the mode of action (Matsumori et al., 2005; Tsuchikawa et al., 2006). However, there have been no synthetic studies enabling investigation of effects of alterations on the polyol part of the molecule from C-2 through to C-11 or at C-15.

Recently, amphotericin analogs have been produced by manipulation of biosynthetic genes in *S. nodosus*. The macrolactone core of amphotericin B is assembled by a modular polyketide synthase (PKS) (Caffrey et al., 2001). Each extension module contains acyltransferase (AT), 3-oxoacylsynthase (KS), and acyl carrier protein (ACP) domains that generate a new 3-oxoacyl intermediate. In most cycles, 3-oxoacyl reductase (KR) domains catalyze formation of 3-hydroxyacyl groups. Dehydratase (DH) domains may then catalyze dehydration of 3-hydroxyacyl chains to form 2-enoyl intermediates which may be further reduced by enoyl reductase (ER) domains. *S. nodosus* produces a mixture of the heptaene amphotericin B (**1**) and the tetraene amphotericin A (**2**) (Figure 1), suggesting that the ER5 domain only acts on some of the nascent oligoketide chains. Completed chains lactonize and then undergo three late post-PKS modifications:

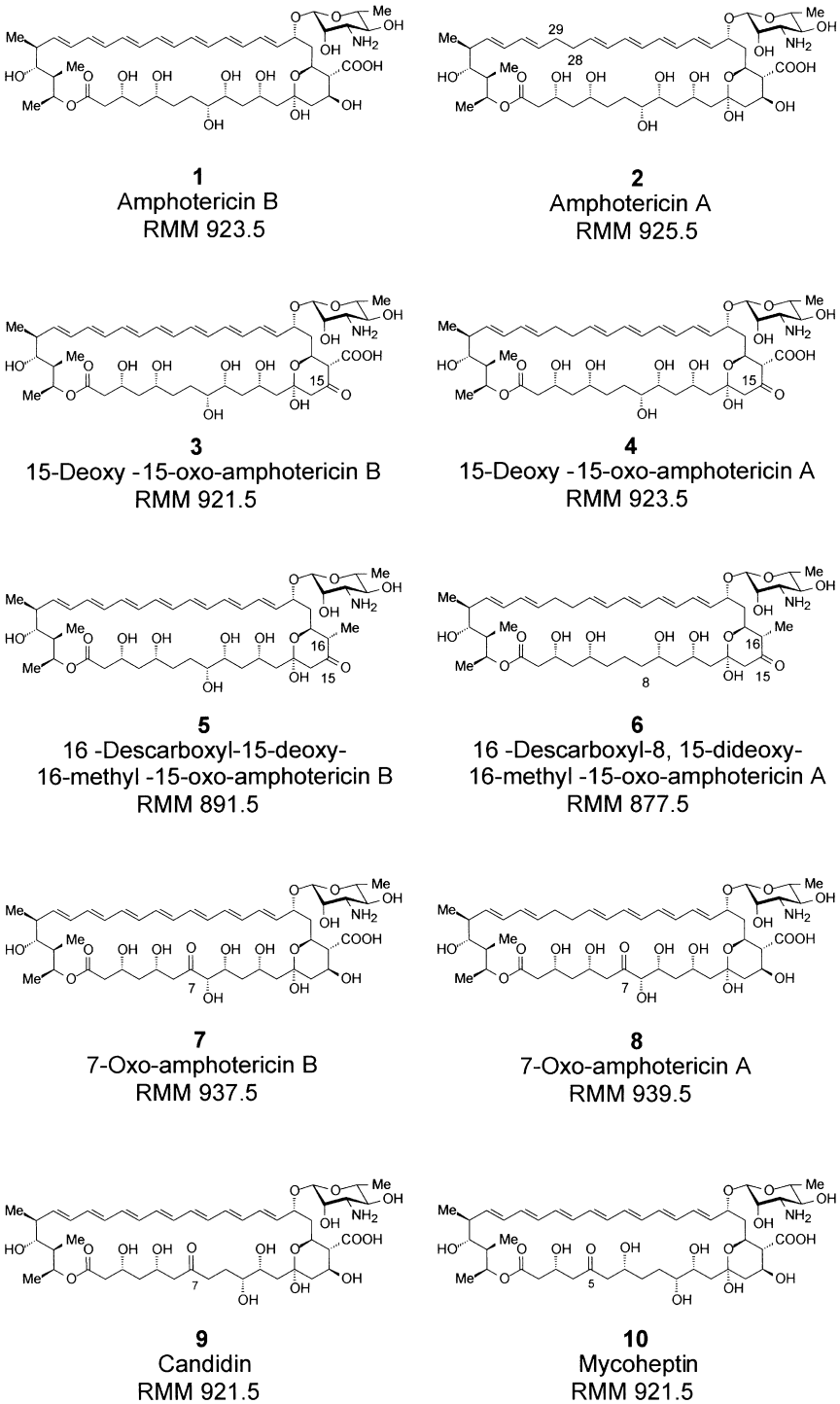

Figure 1. Structures and Relative Molecular Masses of Amphotericin B, Amphotericin Analogs, and Related Polyenes

a methyl branch at C-16 is oxidized to a carboxyl group by a cytochrome P450, a mycosaminyl sugar residue is attached at C-19, and a hydroxyl group is introduced at C-8 (Byrne et al., 2003).

The first analogs generated by engineered biosynthesis were obtained by inactivation of late genes. Similar work has been carried out on the streptomycetes that produce the related polyenes pimaricin, nystatin, candicidin, and rimocidin (Aparicio et al., 2003; Seco et al., 2005). De-epoxypimaricin, 10-deoxy-nystatin, and 8-deoxy-amphotericin B, obtained by inactivation of cytochrome P450 hydroxylase genes, retained antifungal activity (Mendes et al., 2001; Volokhan et al., 2006; Byrne et al., 2003). Disruption of an *S. nodosus* gene encoding a different cytochrome P450 resulted in 16-descarboxyl-16-methyl-amphotericins that retained antifungal activity and had low hemolytic activity (Carmody et al., 2005). Similar improvements were also seen with rimocidin and tetraene CE-108 derivatives that have amide or methyl groups in place of exocyclic carboxyl groups (Seco et al., 2005). Disruption of mycosamine biosynthetic genes gave the aglycone 8-deoxy-amphoteronolide A (Byrne et al., 2003) and an analog glycosylated with a neutral deoxyhexose (Carmody et al., 2005).

New polyenes have also been generated by engineering PKS genes. A pentaene analog of amphotericin B was inactive (Carmody et al., 2004), and a hexaene derivative of nystatin had reduced activity (Brautaset et al., 2002). Zotchev and coworkers introduced hydroxyl groups into the polyene unit of nystatin by inactivating DH3 and DH4 of the PKS. The resulting 33- and 35-hydroxy-nystatins showed increased water solubility but dramatically reduced antifungal activity (Borgos et al., 2006).

This study aimed to explore further the range of analogs that can be obtained by genetic engineering. Inactivation of PKS KR domains has the effect of replacing alkane, alkene, or hydroxyl groups with ketone groups. These analogs will be useful in investigating structure-activity relationships and also because newly introduced carbonyl groups can be chemically modified to introduce a wide range of steric, solvation, or electronic alterations to the molecule. The various KR domains in the amphotericin PKS were considered to identify optimal targets for inactivation. The hydroxyl groups introduced by many of these domains are essential for macrolactone formation (KR1), biosynthesis of the polyene unit (KR3–KR9), glycosylation (KR10), and formation of the hemiketal ring (KR11). The hydroxyl group introduced by KR2 is important for stable transmembrane channel formation (James and Rawlings, 1996). Because modifications of the polyol chain have not been fully investigated,

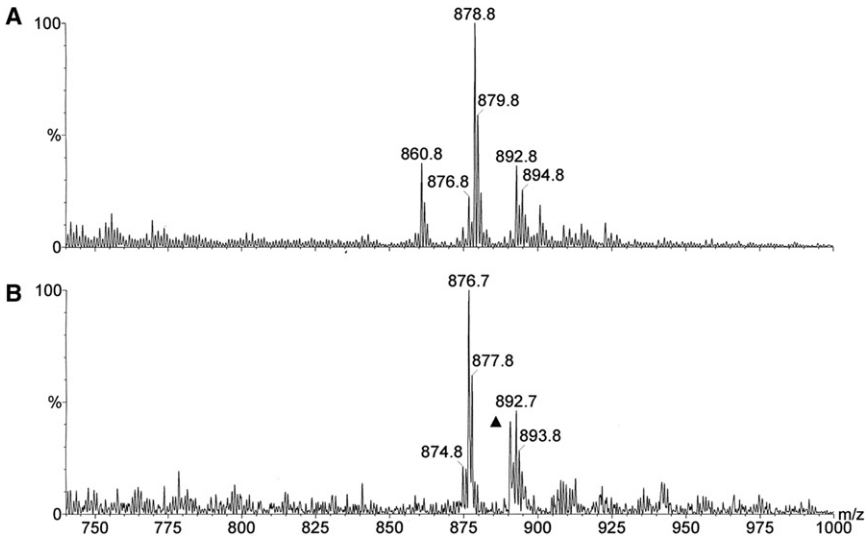

Figure 2. ESMS Analysis of Tetraene-Enriched Extract from *S. nodosus* ΔNM-KR12

Analyses in positive and negative ion modes are shown in (A) and (B), respectively. The major peaks at 878.8 (A) and 876.7 (B) are consistent with 16-descarboxyl-8,15-dideoxy-16-methyl-15-oxo-amphotericin A (**6**) ($[M + H]^+$ = 878.5; $[M - H]^-$ = 876.5). The peaks at 894.8 (A) and 892.7 (B) correspond to the C-8 hydroxylated form of this compound. The peaks at 892.8 (A) and 890.7 ([B], indicated by triangle) correspond to the heptaene 16-descarboxyl-15-deoxy-16-methyl-15-oxo-amphotericin B (**5**).

the domains chosen for initial inactivation were KR12 and KR16. Inactivation of KR12 should give 15-deoxy-15-oxo-amphotericins **3** and **4**, whereas inactivation of KR16 should give 7-oxo-amphotericins **7** and **8** (Figure 1; see also the Supplemental Data available with this article online). This study aimed to investigate whether engineered biosynthesis could deliver these compounds in quantities sufficient for purification, characterization, and bioassay. A ketone group at C-15 would allow chemical modification of the polar end of the molecule, for example to increase the water solubility and decrease the aggregation found in serum. In addition, 15-deoxy-15-oxo-amphotericins might decarboxylate chemically to yield useful analogs with no substituent at C-16. Introduction of a ketone group at C-7 would allow further chemical modifications that could increase the polarity of the polyol chain without eliminating antifungal activity.

RESULTS

Strategy for Inactivation of KR Domains

Studies on other modular PKSs indicate that extensive deletions from PKS domains can result in low product yields, possibly because correct folding of the multienzyme polypeptides is impaired. Point mutations that replace active site residues can inactivate domains without causing structural disruption. Reid and coworkers inactivated KR6 in 6-deoxy-erythronolide B synthase by replacing an active site tyrosine with phenylalanine, and obtained good yields of the expected 3-oxo analog (Reid et al., 2003). Here, this approach was used with the amphotericin PKS. The KR12 domain is located within the hexamodular AmphI protein and the KR16 domain is located within the trimodular AmphJ protein. The strategy for KR12 inactivation aimed to change the DNA sequence around the active site tyrosine codon from GGC-AAC-TAC to GGA-AGC-TTC. This would replace the TAC codon (for tyrosine 6165 of AmphI) with TTC for phenylalanine. Introduction of a HindIII restriction site (AAGCTT) changes the preceding GGC-AAC codons for glycine and asparagine to GGA-AGC for glycine and serine. The asparagine → serine change was expected to be neutral because many KR domains have serine at this position (Caffrey, 2003). A similar strategy was designed for inactivation of KR16. The aim was to replace the GCC-AAC-TAC sequence around the active site tyrosine codon (tyrosine 720 of AmphJ) with GCA-AGC-TTC. This would introduce the same changes as those in the mutated KR12 coding sequence, except that a GCA alanine codon replaces a GCC alanine codon. Introduction of GGA and GCA codons was not expected to impair translation of PKS genes because *amphI* contains 68 GGA codons and *amphJ* contains 19 GCA codons.

PCR mutagenesis was used to construct plasmids containing the engineered KR12 and KR16 coding sequences. The details of these constructions are shown in Figures S1–S3. The two mutated DNA sequences were cloned into phage KC-UCD1 to give recombinant phages KC-KR12 and KC-KR16. These were used to introduce the engineered DNA into *S. nodosus* to allow gene replacement by homologous recombination.

Inactivation of KR12

Homologous recombination in polyene-producing streptomycetes can be unpredictable (Aparicio et al., 2003; Volokhan et al., 2006), and attempts to replace the KR12 coding sequence in wild-type *S. nodosus* were not successful (see Experimental Procedures). However, this gene replacement was relatively straightforward in strain ΔNM, which lacks the *amphN* cytochrome P450 gene and *amphM* ferredoxin gene and produces 16-descarboxyl-16-methyl-amphotericin B and 8-deoxy-16-descarboxyl-16-methyl-amphotericin A (Carmody et al., 2005). Gene replacement mutants were identified by amplifying the KR12 coding region and by testing for the presence of a HindIII site (Figure S4). The resulting *S. nodosus* ΔNM-KR12 double mutants gave only trace levels of tetraene or heptaene production. Yields were increased by including glycerol (100 mM) and Amberlite XAD16 resin (5% w/v) in the production medium. Under these conditions, the yields were 8 mg tetraene and 4 mg heptaene per liter. The methanolic extract from the sedimentable fraction of the culture was concentrated in vacuo and chromatographed on a Sephadex LH20 column to give a tetraene fraction that contained some heptaene and an impure heptaene fraction that was free of tetraene. Analysis by electrospray mass spectrometry (ESMS) (Figure 2) indicated that the tetraene-enriched fraction contained a major species with a mass appropriate for 16-descarboxyl-8,15-dideoxy-16-methyl-15-oxo-amphotericin A (**6**) ($[M + H]^+$ = 878.8; $[M - H]^-$ = 876.7). A dehydrated form of **6**

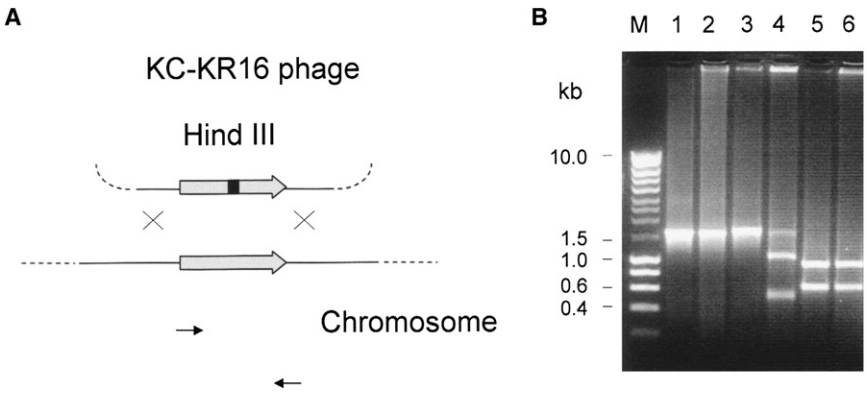

Figure 3. Replacement of the KR16 Coding Sequence in *S. nodosus*

(A) The KC-KR16 phage was used to replace the chromosomal sequence with the engineered sequence via two homologous recombination events. (B) Analysis of the KR16 coding region in the chromosome of *S. nodosus* KR16. The KR16 coding region was amplified by PCR with primers KR16checkF and KR16checkR. The PCR products were treated with HindIII and analyzed by agarose gel electrophoresis. Lane M, molecular weight markers. Lanes 1 and 2, material amplified from genomic DNA of *S. nodosus* ATCC14899 and *S. nodosus* ΔKR16; lanes 3 and 4, HindIII digests of DNA amplified from *S. nodosus* and *S. nodosus* ΔKR16. The KR16 sequence (1576 bp) amplified from the wild-type strain was not digested with HindIII (lane 3), whereas the corresponding region from *S. nodosus* ΔKR16 was cut to give 1046 and 526 bp fragments (lane 4). A small amount of uncut DNA in lane 4 results from amplification of the KR5 coding sequence. This KR is also preceded by an ER domain, and the KR16 primers closely match this region. DNA amplified from *S. nodosus* (lane 5) and *S. nodosus* KR16 (lane 6) cut completely with KpnI. The KR5 and KR16 coding regions contain a conserved KpnI site at the same position.

($[M + H]^+$ = 860.8) was detected in positive ion mode only. Minor species had masses appropriate for the C-8 hydroxylated form of **6**, 15-deoxy-16-descarboxyl-16-methyl-15-oxo-amphotericin A ($[M + H]^+$ = 894.8; $[M - H]^-$ = 892.7). The sample also contained peaks appropriate for the heptaene 15-deoxy-16-descarboxyl-16-methyl-15-oxo-amphotericin B (**5**) ($[M + H]^+$ = 892.8; $[M - H]^-$ = 890.7). These peaks were also detected in the heptaene-enriched sample (not shown). No traces of aglycones were detected, suggesting that the introduction of a ketone group at C-15 does not impair glycosylation by AmphDI.

High-resolution ESMS gave the molecular formula $C_{47}H_{75}NO_{14}$ for the major tetraene (observed mass = 878.5284, calculated exact mass for **6**, $[M + H]^+$ = 878.5266). The molecular formula $C_{47}H_{73}NO_{15}$ was obtained for the heptaene (observed mass = 892.5082, calculated exact mass for **5**, $[M + H]^+$ = 892.5058).

A crude sample of **5** had antifungal activity at a concentration of 10 μg/ml and a crude sample of **6** was active at 5 μg/ml. Because 8-deoxy-16-descarboxyl-16-methyl-amphotericin A and 16-descarboxyl-16-methyl-amphotericin B had minimum inhibitory concentrations of 5 μg/ml and 1 μg/ml, respectively, the presence of a ketone group at C-15 causes some loss in antifungal activity.

The yields were not high enough to allow purification of sufficient material for NMR analysis. The purification of amphotericin analogs critically depends on selective precipitation of the polyenes when methanol extracts are concentrated. This separates polyenes from lipids and other contaminants. We have found that when the polyene yield is below 20 mg per liter, polyenes do not precipitate from concentrated extracts. The ratio of contaminants to polyenes remains high, and further purification steps have not yielded material that gives good NMR spectra. However, we have shown that biosynthesis of **5** and **6** is possible and that these compounds still have antifungal activity. Attempts to improve yields will be made in future work.

Complementation of the *amphNM* Deletion

Attempts were made to complement the *amphNM* deletion in the ΔNM-KR12 strain and to generate a strain that would synthesize 15-deoxy-15-oxo analogs **3** and **4** containing a carboxyl group at C-16. The *amphNM* region was amplified from a cosmid clone (Caffrey et al., 2001) by PCR with primers AmphNM-F and AmphNM-R. The PCR product was digested with BglII and HindIII and ligated between the BamHI and HindIII sites of pIAGO (Aguirrezabalaga et al., 2000), downstream from the strong *ermE* promoter, to give pIAGO-*amphNM*. To construct a second expression plasmid pIAGO-*amphM*, which contains only the ferredoxin gene, the amplified DNA was cut with BclI and HindIII and cloned between the BamHI and HindIII sites of pIAGO.

The pIAGO-*amphNM* construct was introduced into strain ΔNM-KR12 and strain ΔNM. Polyenes produced by strain ΔNM containing pIAGO-*amphNM* were purified and analyzed by ESMS. This revealed that the strain produced amphotericins B (**1**) and A (**2**) with a 10-fold increase in yield (ca 500 mg/l) and only traces of the descarboxyl analogs were detected (data not shown). The fact that the plasmid-borne *amphNM* genes complemented the chromosomal *amphNM* deletion showed that the *ermE* promoter is functional in *S. nodosus*. However, no polyenes were produced by *S. nodosus* ΔNM-KR12 containing pIAGO-*amphNM*. This suggests that compounds **3** and **4** might be toxic to producing cells, or unstable, so it might not be possible to obtain 15-oxo-amphotericins in *S. nodosus* strains that retain functional *amphN* and *amphM* genes. Thus, it was not possible in this work to determine whether introduction of a ketone at C-15 could promote loss of an exocyclic carboxyl group by spontaneous decarboxylation.

In control experiments, the empty pIAGO vector had no effect on polyene production by strain ΔNM or strain ΔNM-KR12. A pIAGO construct containing *amphM* alone caused no change in the pattern of polyene production by strain ΔNM.

Inactivation of KR16

The KC-KR16 phage was used to obtain a gene replacement mutant in the wild-type strain (Figure 3). This mutant *S. nodosus* ΔKR16 produced tetraene (200 mg/l) and heptaene (100 mg/l) in yields comparable to those obtained from the wild-type strain. Methanolic extracts of the mycelia were concentrated in vacuo until a yellow precipitate formed that contained mostly heptaene. Sedimentation of this precipitate by centrifugation provided a cleaner separation of the heptaene and tetraene than was

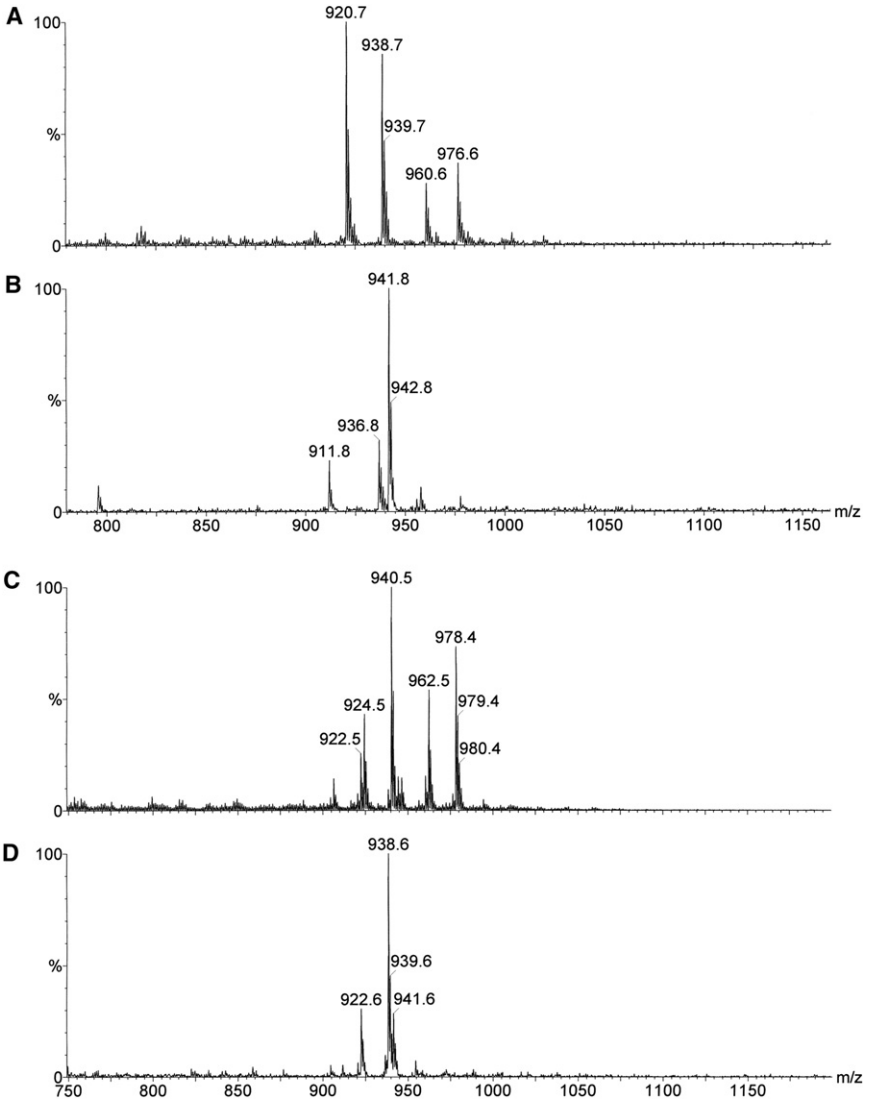

Figure 4. ESMS Analysis of Heptaene and Tetraene Produced by *S. nodosus* KR16

(A) and (B) show analyses of the purified heptaene in positive and negative ion modes. (C) and (D) show analyses of the tetraene in positive and negative ion modes.

(A) Analysis in positive ion mode revealed major species with masses of 938.7, 960.6, and 976.6 consistent with 7-oxo-amphotericin B (**7**), ($[M + H]^+$ = 938.5; $[M + Na]^+$ = 960.5; $[M + K]^+$ = 976.5). An ion corresponding to a dehydrated form of this compound was also detected ($[M + H]^+$ = 920.7).

(B) Analysis in negative ion mode revealed a peak of 936.8 which is also consistent with **7** ($[M - H]^-$ = 936.5). The peaks at 941.8 and 911.8 are contaminants.

(C) Analysis of the tetraene in positive ion mode gave peaks at 940.5, 962.5, and 978.4. These are consistent with 7-oxo-amphotericin A (**8**) ($[M + H]^+$ = 940.5; $[M + Na]^+$ = 962.5; $[M + K]^+$ = 978.4). The peak at 924.5 is consistent with the 8-deoxy analog of **8**, 8-deoxy-7-oxo-amphotericin A ($[M + H]^+$ = 924.5). The peak at 922.5 is a dehydrated form of **8**.

(D) Analysis of the tetraene in negative ion mode revealed peaks at 938.6 corresponding to **8** ($[M - H]^-$ = 938.5) and at 922.6 corresponding to the 8-deoxy analog of **8** ($[M - H]^-$ = 922.5).

achieved with other mutants in earlier studies. The aqueous supernatant was removed and the tetraene was recovered by extraction with a small volume of butanol.

The separated tetraene and the heptaene fractions were dissolved in methanol and further purified by gel filtration on Sephadex LH20. Analysis by ESMS indicated that the major heptaene product was 7-oxo-amphotericin B (**7**) ($[M + H]^+$ = 938.7; $[M + Na]^+$ = 960.6; $[M + K]^+$ = 976.6; $[M - H]^-$ = 936.8) (Figures 4A and 4B). The major tetraene was 7-oxo-amphotericin A (**8**) ($[M + H]^+$ = 940.5; $[M + Na]^+$ = 962.5; $[M + K]^+$ = 978.4; $[M - H]^-$ = 938.6) (Figures 4C and 4D) with low levels of the 8-deoxy analog. Whereas the presence of a ketone group at C-7 will make oxidation at C-8 chemically much more facile, it remains surprising that despite such major adjacent substrate alteration, the AmphL-catalyzed C-8 oxidation of the heptaene is complete, although some of the tetraene was not hydroxylated.

Analysis by high-resolution ESMS gave the molecular formula $C_{47}H_{72}NO_{18}$ for the ΔKR16 heptaene (observed mass = 938.4705, calculated mass for 7-oxo-amphotericin B (**7**), $[M + H]^+$ = 938.4749) and $C_{47}H_{74}NO_{18}$ for the ΔKR16 tetraene (observed mass = 940.4882, calculated mass for 7-oxo-amphotericin A (**8**), $[M + H]^+$ = 940.4906).

Structural Elucidation of 7-Oxo-Amphotericin B

The crude 7-oxo-amphotericin B was converted to the *N*-acetyl methyl ester (**9**) and purified for analysis by 1D and 2D NMR spectroscopy (Figure 5). The carbon NMR shows the expected number of resonances (except for overlapping isochronous resonances in the polyene region), with a resonance at 212.67 ppm confirming a ketone. In the HMBC spectrum, there is a weak crosspeak from this carbon to a hydrogen at 2.68 ppm. The HSQC indicates that the two diastereotopic protons on C-6 are at 2.56 (6a) and 2.68 (6b).

The COSY spectrum shows that H-6a correlated to a C*H*OH resonance at 4.08 assigned as H-5, and that this correlates to two H-4 hydrogens at 1.34 and 1.42, which correlate to H-3 at 4.11, which correlates to H-2 at 2.12 ppm. There are several correlations unobserved such as 35/36, 36/37, 18a/19, and 8/9, presumably due to the dihedral angles involved.

The HSQC shows correlation between the downfield C-O carbon at 79.86 ppm assigned as C-8 and 3.74 ppm (H-8). There is no COSY correlation between H-8 and H-9 assigned as 3.97, which has COSY correlations to both 10a at 1.54 and 10b at 1.58, which correlate with H-11 at 4.13.

The combined NMR spectra (Supplemental Data) are strongly consistent with the expected structure. However, in the absence of an X-ray structure, the large number of near-isochronous

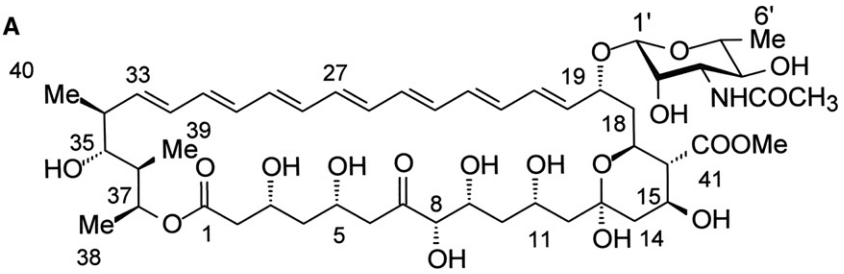

11

Methyl *N*-acetyl-7-oxo-amphotericin B

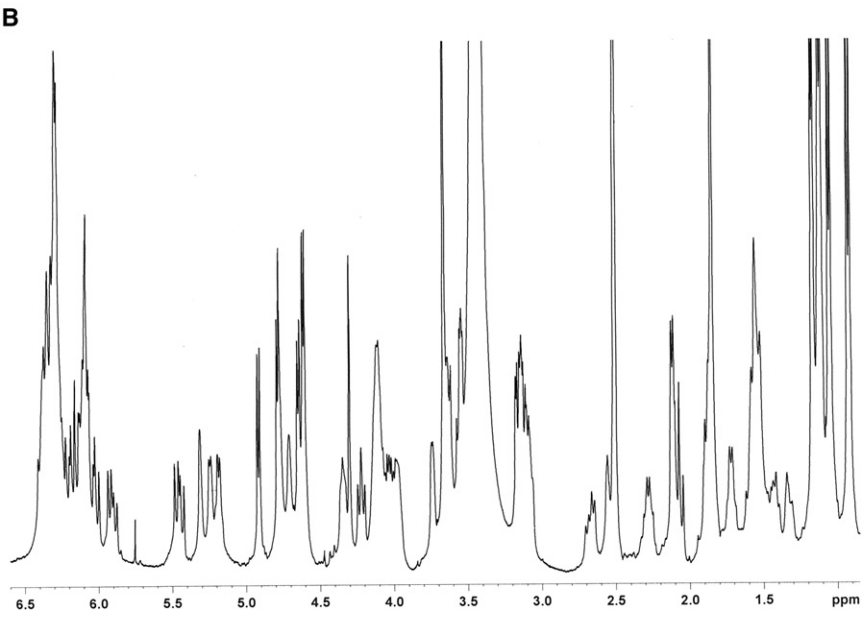

Figure 5. NMR Analysis of 7-Oxo-Amphotericin B

(A) Structure of methyl *N*-acetyl-7-oxo-amphotericin B.

(B) Proton NMR spectrum (400 MHz DMSO-d_6). The amide NH resonance at δ 7.65 ppm is not shown; 2.5 ppm is solvent; 3.5 ppm is water. Full spectra are provided in the Supplemental Data.

resonances in both carbon and proton NMR precludes rigorous exclusion of regioisomers, and is not indicative of stereochemistry, presumed to be as for amphotericin B. Efforts are in progress to obtain further data, and to carry out X-ray crystallographic analysis.

The extra carbonyl group at C-7 might have a small through-space or conformational effect upon the polyene region in the proton NMR. In amphotericin itself there is a resonance slightly downfield of the other polyenes, whereas in our derivatized product this has merged into the other polyene resonances.

Analysis of Antifungal and Hemolytic Activities of 7-Oxo-Amphotericins

For assessment of antifungal and hemolytic activities, unmodified 7-oxo-amphotericin B was purified further. Purification by reverse-phase HPLC yielded material that was 87.5% pure. In control assays, amphotericin B (**1**) showed a minimum inhibitory concentration (MIC) of 1.25 μg/ml and a minimum hemolytic concentration (MHC) of 6 μg/ml. 7-oxo-amphotericin B (**7**) had a lower antifungal activity (MIC = 4.5 μg/ml) but showed a greater relative decrease in hemolytic activity (MHC = 65 μg/ml). Surprisingly, tests with the tetraene 7-oxo-amphotericin A (**8**) could detect neither antifungal activity (MIC > 166 μg/ml) nor hemolytic activity (MHC > 96 μg/ml). Further work on the conformation of this compound will be necessary to explain this result.

DISCUSSION

In recent years there has been a dramatic increase in life-threatening systemic mycoses, and the emergence of resistance to current antibiotic treatments is leading to a crisis in antifungal therapy (Lemke et al., 2005). Because resistance to amphotericin B apparently does not readily arise in fungal pathogens (Abu-Salah, 1996; Hamilton-Miller, 1973), there is considerable interest in identifying amphotericin analogs with reduced toxicity. Such analogs could also be used for treatment of other diseases.

This work has yielded four amphotericin derivatives: **5**, **6**, **7**, and **8**. As yet, it has not been possible to engineer the biosynthesis of analogs **3** and **4**. However, sufficient **6** was obtained to show that a ketone group at C-15 does not impair antifungal activity. A ketone group at this position will allow derivatization for production of interesting semisynthetic analogs that have not been accessible before. Work is in progress to improve the yields of compounds **5** and **6** by random mutagenesis and by investigating fermentation conditions.

The nonaromatic heptaenes candidin and mycoheptin have ketone groups at the carbon atoms corresponding to C-7 and C-5 of amphotericin B, respectively (Pawlak et al., 1993; Omura and Tanaka, 1986) (Figure 1). The 7-oxo-amphotericin B analog (**7**) is structurally related to these heptaenes but has a novel extra hydroxyl group in the polyol chain adjacent to the ketone. The antifungal activities of candidin and mycoheptin are comparable to that of amphotericin B (Thomas, 1976). Candidin is less hemolytic than amphotericin B (Cybulska et al., 1995). Mycoheptin is slightly less active than amphotericin B at promoting cation efflux from muscle cells (Shvinka and Caffier, 1994). Otherwise, little is known about the biological activities of these heptaenes. Although 7-oxo-amphotericin B had a lower antifungal activity than amphotericin B, it showed a greater reduction in hemolytic activity and might be of some therapeutic interest. The additional ketone group should increase the polarity of the polyol chain. Selective chemical modification of this group should allow manipulation of the transmembrane channel. It might be possible

to achieve stereospecific reduction of the ketone group by chemical means.

The 7-oxo-amphotericin A analog (**8**) showed a complete loss of antifungal activity. This is surprising, because the polyene unit of this analog is identical to that of nystatin, which is highly active. However, some semisynthetic amphotericin derivatives are not antifungal but retain membrane-permeabilizing activity (Zumbuehl et al., 2004). This suggests that loss of antifungal activity might not necessarily mean loss of other potentially useful biological activities. The 7-oxo-amphotericins A and B have increased water solubility and reduced hemolytic activities. These analogs are synthesized in high yields, are easily separated, and can be obtained in quantities sufficient for testing against parasites, pathogenic prion proteins, and viruses.

SIGNIFICANCE

This work shows that the introduction of a ketone group at C-15 does not abolish the antifungal activity of amphotericin B. Increased yields of these 15-deoxy-15-oxo analogs should provide starting material for a range of interesting semisynthetic derivatives. Introduction of ketone groups at C-7 did not impair C-8 hydroxylation, so that 7-oxo-amphotericins A and B were biosynthesized in good yield. The 7-oxo-amphotericin B analog showed decreased hemolytic activity and retained antifungal activity. These 7-oxo analogs can now be purified in quantities sufficient for testing in different therapeutic areas.

EXPERIMENTAL PROCEDURES

DNA Methods

Escherichia coli XL-Blue 1 was used as a host for construction of plasmids. Deep Vent, a high-fidelity DNA polymerase, was used for PCR. Resequencing of amplified DNA was carried out by MWG Biotech. Recombinant phages were constructed as described previously (Carmody et al., 2004), with KC-UCD1 as the vector and *Streptomyces lividans* 1326 as host. These phages were used to infect *S. nodosus* and *S. nodosus* ΔNM (Carmody et al., 2005). When engineered DNA is introduced into the host cell, a double-crossover recombination event is required to bring about gene replacement. In practice, two single-crossover events have to be identified separately. The first recombination between phage and chromosomal sequences brings about integration of phage DNA to form a prophage. The host cell becomes a lysogen that can be selected because the phage vector includes a thiostrepton-resistance gene. A phage repressor switches off phage lytic genes. The homologous phage-borne and chromosomal sequences are duplicated, in direct repeat orientation, within the lysogen. A second recombination between these sequences results in excision of the prophage, loss of thiostrepton resistance, and either gene replacement or reversion to the parental genotype. In this work, lysogens were subcultured three times in the absence of antibiotic. Protoplasts were prepared to separate individual cells from mycelial networks. Colonies derived from regenerated protoplasts were screened for thiostrepton sensitivity to identify recombinants that had lost the prophage. To identify gene replacement mutants, the KR coding sequences were amplified and tested for the presence of a HindIII site.

The KC-KR12 phage gave lysogens on both *S. nodosus* and *S. nodosus* ΔNM. Sixteen thiostrepton-sensitive revertants were obtained by screening 80 clones derived from the *S. nodosus* ΔNM::KC-KR12 lysogen. Four of these revertants were gene replacement mutants (Figure S4). Over 250 revertants of the *S. nodosus*::KC-KR12 lysogen were tested, but all of these had undergone reversion to wild-type.

The KC-KR16 phage gave a lysogen on *S. nodosus*. Forty thiostrepton-sensitive revertants were obtained after screening 100 regenerated protoplasts. Screening of ten revertants yielded six gene replacement mutants.

Oligonucleotides AmphNM-F (5′-TGACAGATCTGGACCAGGAGTTCATCA CCG-3′) and AmphNM-R (5′-AAAAAAGCTTGATGTCCTGCTGATCGATCGGA TGTGGCT-3′) were used to amplify the *amphNM* region for subcloning. Oligonucleotides KR16checkF (5′-TGTTCCTCACCGCTTACCACGCGCTGAA-3′) and KR16checkR (5′-AGCTCGATCGCGGTGAGCGAGTCGAA-3′) were used to amplify the KR16 coding region to identify mutants.

pIAGO is a bifunctional (*Streptomyces-E. coli*) plasmid that contains the promoter of the erythromycin resistance gene (*ermE*) from *Saccharopolyspora erythraea* (Aguirrezabalaga et al., 2000). It confers thiostrepton resistance in *Streptomyces* and ampicillin resistance in *E. coli*. Transformation of *S. nodosus* protoplasts was carried out as described in Kieser et al. (2000).

Initial Characterization of Polyene Products

For purification and analysis of polyenes, *S. nodosus* strains were grown on fructose-dextrin (15% soluble) soya flour medium (McNamara et al., 1998) containing Amberlite XAD16 (5% w/v). For the ΔNM-KR12 mutant, 100 mM glycerol was included (Recio et al., 2006). Cultures (500 ml in 2 l flasks) were shaken (200 rpm) at 30°C for up to 5 days. Mycelia and Amberlite resin were sedimented by centrifugation and polyenes were extracted from the pellet with methanol (100 ml per 500 ml culture). Polyene concentrations were determined by spectrophotometry as described previously (Carmody et al., 2005). Methanol extracts were concentrated by rotary evaporation. Polyenes precipitating from the aqueous residue were sedimented by centrifugation and dissolved in a small volume of methanol; those remaining in the aqueous layer were extracted into a small volume of butanol. Polyenes were then partially purified by chromatography on a Sephadex LH20 column equilibrated with methanol (Carmody et al., 2005).

Electrospray mass spectrometry (ESMS) was carried out with a Quattro Micro tandem quadrupole mass spectrometer (Waters Ltd., Manchester, UK) in positive and negative ionization modes. Exact mass measurements were determined using an online LCT (liquid chromatography to a time of flight) instrument (Waters Ltd.). The electrospray mass spectra were acquired on the LCT, equipped with a lockspray interface, in the positive ion mode. The samples were introduced into the ion source by an LC system (Waters Alliance 2795, Waters Ltd.) in acetonitrile:water (60:40 v/v) at 200 μl/min. The LCT was externally calibrated for the mass range m/z 100 to m/z 1000. A lock (reference) mass (m/z 556.2771) was used.

Antifungal and hemolytic activities were assessed as described previously (Carmody et al., 2005). For assessment of these biological activities, unmodified 7-oxo-amphotericin B (**7**) was further purified by reverse-phase HPLC on a Supelco C_{18} column (5 μm, 21.2 mm diameter, 25 cm length). The polyene was eluted with a gradient of 70% methanol, 30% 50 mM citrate (pH 5. 3) to 100% methanol over 12 min at a flow rate of 20 ml/min. The peak fraction was dried down, redissolved in 50% (v/v) methanol, and desalted using HP20 anion-exchange resin. The final material (3.2 mg dry weight) gave a single peak when rechromatographed on an analytical scale (Supplemental Data) and was 87.5% pure as determined by gravimetric measurements.

Purification and Characterization of Methyl *N*-Acetyl-7-Oxo-Amphotericin B

The KR16 mutant was grown as above (in 16 × 250 ml volumes of production media containing 5% [w/v] Amberlite XAD16 resin in trigrooved 2 l flasks). The combined mycelia and beads were extracted with methanol (2 × 2l). UV assay emonstrated the presence of heptaenes (350 mg) and tetraenes (1.4 g). The combined methanolic extracts were concentrated in vacuo until a yellow precipitate formed which was collected and washed with water (15 ml) to give heptaenes (135 mg) and tetraenes (57 mg) in a yellow powder (350 mg). DMSO (2 ml) and methanol (2 ml) were added to the resulting dried pellet and the reaction mixture was cooled to 0°C. Then acetic anhydride (0.041 ml) was added dropwise and the reaction mixture was allowed to warm to room temperature with stirring (1 hr) and then diluted with methanol (200 ml). Excess ethereal diazomethane was added, and after concentration in vacuo addition of excess ether yielded heptaenes (113 mg) and tetraenes (27 mg) as a yellow powder (195 mg). The crude product was adsorbed onto silica gel (40–63 μm; 50 g), and purified by flash silica chromatography. The polyene-containing fractions (10%–20% MeOH in EtOAc) were combined and purified twice by HPLC (Varian Prostar diode array with a Supelco silica column (5 μm, 21.2 mm diameter, 25 cm length, 20 ml/min flow), methanol/dichloromethane 5%–15% gradient,

to give methyl *N*-acetyl 7-oxo-amphotericin B (35 mg) as a single peak ca 97% pure.

The physical properties were as follows: R_f 0.47 (silica, 20% MeOH in DCM); IR (powder) ν_{max} 3346 (s, OH), 1722 (s, C = O, ester, lactone, 7-oxo), 1653 (s, C = O, *N*-acetate); UV-vis (MeOH) λ_{max} 406 (59,700), 383 (56,160), 364 (33,220), 346 (15,380); m/z (ESI) = 992.4 [$(M - H)^-$, 20%]; 1028.6 [$(M + Cl^-)^-$, 100%]; $C_{50}H_{74}NO_{19}$ $(M - H)^-$, 992.48551; found, 992.48248.

NMR spectra were recorded on a Bruker DRX 400 spectrometer with resonance frequencies quoted in parts per million relative to tetramethylsilane. Standard parameters were used for 1D and 2D NMR spectra, which included ^1H, ^{13}C (with attached proton test), $^1H/^1H$-correlated spectroscopy (COSY), heteronuclear single-quantum coherence (HSQC), and heteronuclear multiple-bond correlation (HMBC). Full spectra and parameters used are shown in Supplemental Data.

^1H NMR (400 MHz DMSO-d_6) δ 7.65 (d, 1H, *J* 8.2, NH), 6.47–6.04 (m, 10 H, H-22 → H-31), 6.11 (m, 1H, H-21), 6.08 (m, 1H, 13-OH), 6.03 (t, 1H, *J* 10.1, H-32), 5.91 (dd, 1H, *J* 8.7, 15.1, H-20), 5.45 (dd, 1H, *J* 10.1, 15.5, H-33), 5.31 (s, 1H, 3-OH), 5.24 (d, 1H, *J* 5.5, 8-OH), 5.19 (m, 1H, H-37), 4.91 (d, 1H, *J* 6.3, 15-OH), 4.79 (d, 1H, *J* 5.6, 4′-OH), 4.77 (m, 1H, 11-OH), 4.71 (m, 1H, 5-OH), 4.65 (d, 1H, *J* 6.3, 35-OH), 4.61 (d, 2H, *J* 5.2, 2′-OH, 9-OH), 4.35 (m, 1H, H-19), 4.30 (s, 1H, H-1′), 4.22 (t, 1H, *J* 9.5, H-17), 4.13 (m, 1H, H-11), 4.11 (m, 1H, H-3), 4.09 (m, 1H, H-5), 4.03 (dq, 1H, *J* 5.5, 10.5, H-15), 3.97 (m, 1H, H-9), 3.74 (br d, 1H, *J* 3.5, H-8), 3.66 (s, 3H, OMe), 3.62 (m, 1H, H-3′), 3.54 (m, 1H, H-2′), 3.16 (m, 1H, H-5′), 3.12 (m, 1H, H-4′), 3.08 (m, 1H, H-35), 2.68 (dd, 1H, *J* 8.6, 10.6, H-6b), 2.56 (m, 1H, H-6a), 2.28 (dq, 1H, *J* 6.1, 15.5, H-34), 2.12 (ca d, 2H, *J* 5.8, H-2ab), 2.07 (t, 1H, *J* 10.5, H-16), 1.87 (m, 1H, H-14b), 1.86 (m, 1H, H-18b), 1.85 (s, 3H, NHCOCH_3), 1.72 (q, 1H, *J* 6.9, H-36), 1.63 (m, 1H, H-12b), 1.58 (m, 1H, 10b), 1.56 (m, 1H, 18a), 1.56 (m, 1H, 12a), 1.55 (m, 1H, 10a), 1.42 (m, 1H, H-4b), 1.34 (m, 1H, H-4a), 1.16 (d, 3H, *J* 5.5, 6′-CH_3), 1.12 (m, 1H, H-14a), 1.11 (d, 3H, *J* 6.4, 38-CH_3), 1.05 (d, 3H, *J* 6.4, 40-CH_3), 0.92 (d, 3H, *J* 6.9, 39-CH_3); ^{13}C NMR (100.62 MHz DMSO-d_6) δ 212.67 (C-7), 173.28 (C-41), 171.09 (C-1), 169.74 (NHC[O]CH_3), 137.16 (C-33), 136.31 (C-20), 134.67, 134.56, 133.90, 132.58 (2 C), 132.48 (2 C), 132.35 (C-21), 131.55 (C-32), 129.9, 97.88 (C-13), 97.31 (C-1′), 79.86 (C-8), 78.05 (C-35), 75.00 (C-19), 74.03 (C-5′), 70.32 (C-9), 70.14 (C-4′), 69.52 (C-2′), 69.44 (C-37), 66.36 (C-3), 65.84 (C-11), 65.69 (C-15), 65.60 (C-17), 57.44 (C-16), 55.45 (C-3′), 52.04 (OCH_3), 47.57 (C-6), 46.48 (C-12), 44.60 (C-14), 44.05 (C-4), 43.13 (C-34), 42.54 (C-2), 41.33 (C-10), 37.17 (C-18), 23.26 (NHC[O]CH_3), 18.94 (C-40), 18.59 (C-6′), 17.51 (C-38), 12.72 (C-39).

COSY correlations: 2/3 (H-2 to H-3), 3/4ab, 4ab/5, 5/6a, 5/6b(w), 8/8-OH, 9/10a, 9/10b(w), 9/9-OH, 10ab/11, 11/12ab, 14a/14b, 14a/15, 14b/15(w), 15/16, 15/15-OH, 16/17, 17/18a, 18b/19(w), 19/20, 32/33, 33/34, 34/40, 34/35, 36/39, 37/38, 3′/4′, 5′/6′.

HSQC (single-bond carbon/proton) correlations: 17.51/1.11 (C/H-38), 18.59/1.16 (6′), 18.94/1.05 (40), 23.26/1.85 (NHCO*Me*), 37.17/1.56 and 1.87 (18), 40.05/1.72 (36), 41.33/1.55 and 1.58 (10), 42.54/2.12 (2), 43.13/2.28 (34), 44.05/1.34 and 1.42 (4), 44.60/1.12 and 1.87 (14), 46.48/1.56 (12), 47.57/2.56 and 2.68 (6), 52.04/3.66 (COO*Me*), 55.45/3.62 (3′), 57.44/2.07 (16), 65.60/4.22 (17), 65.69/4.03 (15), 65.84/4.08 (5), 66.30/4.11 (3), 66.36/4.13 (11), 69.44/5.19 (37), 69.52/3.54 (2′), 70.14/3.12 (4′), 70.32/3.97 (9), 74.03/3.16 (5′), 75.00/4.35 (19), 78.05/3.08 (35), 79.86/3.74 (8), 97.31/4.30 (1′), 129.9/6.09 (polyene), 131.55/6.02 (32), 132–135/6.1–6.43 (polyene), 132.35/6.11 (21), 134.56/6.39 (unknown), 136.31/5.91 (20), 137.16/5.45 (33).

HMBC (multiple-bond carbon/proton) correlations: C7/H6a(w), C13/13(OH), C14/13(OH), C15/H14a, C17/H16, C17/H18b(very weak), C19/H21, C33/H40, C34/H40, C35/H39, C35/H40, C36/H38, C36/H39, C37/H39, C39/H38(w), C4′/H6′, C5′/H6′, -N*HC*OMe, -NHCOCH_3, -*COOC*H_3, -*CHCOOC*H_3.

Supplemental Data

Supplemental Data include 31 figures and 1 table and can be found with this article online at http://www.chembiol.com/cgi/content/full/15/1/78/DC1/.

ACKNOWLEDGMENTS

This work was supported by a grant to P.C. from the Irish Higher Education Authority Programme for Research in Third Level Institutions (PRLTI cycle 3) and a grant to B.R. from the Biotechnology and Biosciences Research Council, UK. B.R. would like to acknowledge valuable assistance from Dr. G. Griffiths and Dr. Graham Eaton in running NMR and mass spectra, respectively, and technical assistance from Michael Lee.

Received: August 1, 2007
Revised: November 16, 2007
Accepted: November 21, 2007
Published: January 25, 2008

REFERENCES

Abu-Salah, K.M. (1996). Amphotericin B: an update. Br. J. Biomed. Sci. *53*, 122–133.

Aguirrezabalaga, I., Olano, C., Allende, N., Rodriguez, L., Braña, A.F., Méndez, C., and Salas, J.A. (2000). Identification and expression of genes involved in biosynthesis of L-oleandrose and its intermediate L-olivose in the oleandomycin producer *Streptomyces antibioticus*. Antimicrob. Agents Chemother. *44*, 1266–1275.

Aparicio, J.F., Caffrey, P., Gil, J., and Zotchev, S.B. (2003). Polyene antibiotic biosynthesis gene clusters. Appl. Microbiol. Biotechnol. *61*, 179–188.

Borgos, S.E.F., Tsan, P., Sletta, H., Ellingsen, T.E., Lancelin, J.M., and Zotchev, S.B. (2006). Probing the structure-function relationship of polyene macrolides: engineered biosynthesis of soluble nystatin analogues. J. Med. Chem. *49*, 2431–2439.

Brautaset, T., Bruheim, P., Sletta, H., Hagen, L., Ellingsen, T.E., Strom, A.R., Valla, S., and Zotchev, S.B. (2002). Hexaene derivatives of nystatin produced as a result of an induced rearrangement within the *nysC* polyketide synthase gene in *S. noursei* ATCC 11455. Chem. Biol. *9*, 367–373.

Byrne, B., Carmody, M., Gibson, E., Rawlings, B., and Caffrey, P. (2003). Biosynthesis of deoxyamphotericins and deoxyamphoteronolides by engineered strains of *Streptomyces nodosus*. Chem. Biol. *10*, 1215–1224.

Caffrey, P. (2003). Conserved amino acid residues correlating with ketoreductase stereospecificity in modular polyketide synthases. ChemBioChem *4*, 654–657.

Caffrey, P., Lynch, S., Flood, E., Finnan, S., and Oliynyk, M. (2001). Amphotericin biosynthesis in *Streptomyces nodosus*: deductions from analysis of polyketide synthase and late genes. Chem. Biol. *8*, 713–723.

Carmody, M., Byrne, B., Murphy, B., Breen, C., Lynch, S., Flood, E., Finnan, S., and Caffrey, P. (2004). Analysis and manipulation of amphotericin biosynthetic genes by means of modified phage KC515 transduction techniques. Gene *343*, 107–115.

Carmody, M., Murphy, B., Byrne, B., Power, P., Rai, D., Rawlings, B., and Caffrey, P. (2005). Biosynthesis of amphotericin derivatives lacking exocyclic carboxyl groups. J. Biol. Chem. *280*, 34420–34426.

Cereghetti, D.M., and Carreira, E.M. (2006). Amphotericin B: 50 years of chemistry and biochemistry. Synthesis (Stuttg) *6*, 914–942.

Cheron, M., Cybulska, B., Mazerski, J., Gryzbowska, J., Czerwinski, A., and Borowski, E. (1988). Quantitative structure-activity relationships in amphotericin B derivatives. Biochem. Pharmacol. *37*, 827–836.

Cybulska, B., Bolard, J., Seksek, O., Czerwinski, A., and Borowski, E. (1995). Identification of the structural elements of amphotericin B and other polyene macrolide antibiotics of the heptaene group influencing the ionic selectivity of the permeability pathways formed in the red cell membrane. Biochim. Biophys. Acta *1240*, 167–178.

Ehrenfreund-Kleinman, T., Azzam, T., Falk, R., Polacheck, I., Golenser, J., and Domb, A.J. (2002). Synthesis and characterization of novel water soluble amphotericin B-arabinogalactan conjugates. Biomaterials *23*, 1327–1335.

Hamilton-Miller, J.M.T. (1973). Chemistry and biology of the polyene macrolide antibiotics. Bacteriol. Rev. *37*, 166–196.

Hartsel, S., and Bolard, J. (1996). Amphotericin B: new life for an old drug. Trends Pharmacol. Sci. *17*, 445–449.

James, P.R., and Rawlings, B.J. (1996). Probing the mechanism of action of amphotericin B. Bioorg. Med. Chem. Lett. *6*, 505–508.

Jones, J., Kosloff, B.R., Benviste, E.N., Shaw, G.M., and Kutsch, O. (2005). Amphotericin-B-mediated reactivation of latent HIV-1 infection. Virology *331*, 106–116.

Kieser, T., Bibb, M.J., Buttner, M.J., Chater, K.F., and Hopwood, D.A. (2000). Introduction of DNA into *Streptomyces*. In Practical *Streptomyces* Genetics, T. Kieser, M.J. Bibb, M.J. Buttner, K.F. Chater, and D.A. Hopwood, eds. (Norwich, UK: John Innes Institute), pp. 229–252.

Lemke, A., Kiderlen, A.F., and Kayser, O. (2005). Amphotericin B. Appl. Microbiol. Biotechnol. *68*, 151–162.

Matsumori, N., Umegawa, Y., Oishi, T., and Murata, M. (2005). Bioactive fluorinated derivative of amphotericin B. Bioorg. Med. Chem. Lett. *15*, 3565–3567.

McNamara, C.M., Box, S., Crawforth, J.M., Hickman, B.S., Norwood, T.J., and Rawlings, B.J. (1998). Biosynthesis of amphotericin B. J. Chem. Soc. Perkin Trans. 1, 83–87.

Mendes, M.V., Recio, E., Fouces, R., Luiten, R., Martin, J.F., and Aparicio, J.F. (2001). Engineered biosynthesis of novel polyenes: a pimaricin derivative produced by targeted gene disruption in *Streptomyces natalensis*. Chem. Biol. *8*, 635–644.

Omura, S., and Tanaka, H. (1986). Production, structure and antifungal activity of polyene macrolides. In Macrolide Antibiotics: Chemistry, Biology, and Practice, S. Omura, ed. (New York: Academic Press), pp. 351–404.

Paquet, V., and Carreira, E.M. (2006). Significant improvement of antifungal activity of polyene macrolides by bisalkylation of the mycosamine. Org. Lett. *8*, 1807–1809.

Pawlak, J., Sowiński, P., Borowski, E., and Gariboldi, P. (1993). Stereostructure and NMR characterization of the antibiotic candidin. J. Antibiot. (Tokyo) *46*, 1598–1604.

Recio, E., Aparicio, J.F., Rumbero, A., and Martin, J.F. (2006). Glycerol, ethylene glycol and propanediol elicit pimaricin biosynthesis in the PI-factor defective strain *Streptomyces natalensis* npi287 and increase polyene production in several wild-type actinomycetes. Microbiology *152*, 3147–3156.

Reid, R., Piagentini, M., Rodriguez, E., Ashley, G., Viswanathan, N., Carney, J., Santi, D.V., Hutchinson, C.R., and McDaniel, R. (2003). A model of structure and catalysis for ketoreductase domains in modular polyketide synthases. Biochemistry *42*, 72–79.

Schaffer, C.P. (1984). Polyene macrolides in clinical practice: pharmacology and adverse and other effects. In Macrolide Antibiotics: Chemistry, Biology, and Practice, S. Omura, ed. (New York: Academic Press), pp. 457–507.

Seco, E.M., Fotso, S., Laatsch, H., and Malpartida, F. (2005). A tailoring activity is responsible for generating polyene amide derivatives in *Streptomyces diastaticus* var. 108. Chem. Biol. *12*, 1093–1101.

Shvinka, N., and Caffier, G. (1994). Cation conductance and efflux induced by polyene antibiotics in the membrane of skeletal muscle fibre. Biophys. J. *67*, 143–152.

Szlinder-Richert, J., Mazerski, J., Cybulska, B., Gryzbowska, J., and Borowski, E. (2001). MFAME, *N*-methyl-*N*-D-fructosyl amphotericin B methyl ester, a new amphotericin B derivative of low toxicity: relationship between self-association and effects on red blood cells. Biochim. Biophys. Acta *1528*, 15–24.

Taylor, A.W., Costello, B., Hunter, P.A., McLachlan, W.S., and Shanks, C.T. (1992). Synthesis and antifungal selectivity of new derivatives of amphotericin B modified at the C-13 position. J. Antibiot. (Tokyo) *46*, 486–493.

Thomas, A.H. (1976). Analysis and assay of polyene antifungal antibiotics. Analyst *101*, 321–340.

Tsuchikawa, H., Matsushita, N., Matsumori, N., Murata, M., and Oishi, T. (2006). Synthesis of 28-^{19}F-amphotericin B methyl ester. Tetrahedron Lett. *47*, 6187–6191.

Volokhan, O., Sletta, H., Ellingsen, T.E., Valla, S., and Zotchev, S.B. (2006). Characterisation of the P450 monooxygenase NysL, responsible for C-10 hydroxylation during biosynthesis of the polyene macrolide antibiotic nystatin in *Streptomyces noursei*. Appl. Environ. Microbiol. *72*, 2514–2519.

Zumbuehl, A., Jeannerat, D., Martin, S.E., Sohrmann, M., Stano, P., Vigassy, T., Clark, D.D., Hussey, S.L., Peter, M., Peterson, B.R., et al. (2004). An amphotericin B-fluorescein conjugate as a powerful probe for biochemical studies of the membrane. Angew. Chem. Int. Ed. Engl. *43*, 5181–5185.

